

13th CIRP conference on Computer Aided Tolerancing

Hydrostatic worktable performance of an ultra-precision optical aspheric machine tool

Shuming Yang^{a,*}, Pu Zhao^a, Yukun Xu^a, Lin Sun^a, Pengfei Wu^a, Xingyuan Long^a, Zhuangde Jiang^a

^aState Key Laboratory of Mechanical Manufacturing Systems Engineering, Xi'an Jiaotong University, Xi'an, 710049, China

* Shuming Yang. Tel.: +86-029-82668616; E-mail address: shuming.yang@mail.xjtu.edu.cn.

Abstract

Hydrostatic guide-ways utilizing thin film feedback restrictor are applied for the ultra-precision optical aspheric machine tool that we have developed. This machine tool. The parameters of the PM flow controllers have a direct influence on the dynamic performance of the hydrostatic worktable. During the machining process, the cutting force acted on the cutting tool and other load will be transferred to the hydrostatic guide-way. On the basis of the flow equation of the PM controller and the force schematic of the hydrostatic worktable, this paper theoretically establishes a mathematic model of the hydrostatic guide-ways of the worktable. The transfer function is derived, and the influence of the restrictor parameters, including the initial flow rate, oil film thickness, pump pressure and initial flow ratio, on the dynamic performance of the hydrostatic guide-way is studied. According to the results, it needs the longest time at the flow rate ratio K_r of 5 for the hydrostatic bearing system to adjust and the maximum displacement and the maximum overshoot arose. When the flow rate of the restrictor reaches $20\text{cm}^3/\text{s}$, the overshoot and response time of the hydrostatic guide-way bearing system hardly increase. The final displacement of the system decreases when the pump pressure increases. The effect of pump pressure increase provides a decrease in the final displacement of the system.

© 2015 The Authors. Published by Elsevier B.V. This is an open access article under the CC BY-NC-ND license

(<http://creativecommons.org/licenses/by-nc-nd/4.0/>).

Peer-review under responsibility of the organizing committee of 13th CIRP conference on Computer Aided Tolerancing

Keywords: Ultra-precision machine tool, hydrostatic guides, mathematical model, dynamic characteristic

1. Introduction

The flow equation of the PM flow controller is

$$Q_r(P_r) = Q_0[1 + (K_r - 1)P_r/P_s] \quad (1)$$

where P_s is the pump pressure, P_r is the oil chamber pressure under any load, Q_r is the flow of the chamber when the chamber pressure is P_r , K_r is the flow ratio and $K_r = Q_p/Q_0$, Q_p is the oil flow when $P_r = P_s$, Q_0 is the oil flow when $P_r = 0$.

The external load on the worktable is variable, so the pressure of the oil pockets needs be adjustable by the hydrostatic bearing system. The relationship between the external load incentive and the dynamic performance of the hydrostatic bearing system has been studied [12]. The dynamic characteristic simulation of the hydrostatic transmission system has been discussed based on the mathematic model using Matlab in paper [13]. However, the

hydrostatic bearing system is studied by the linearized nonlinear differential equations to acquire the transformation function of the system.

This paper aims to study the effect of the parameter of PM controller on the dynamic performance of the closed hydrostatic guide-way worktable. According the force schematic of the closed hydrostatic bearing system, both the mathematic model of the hydrostatic model and the transformation function of the system are derived to take account the parameters of the PM controller. The dynamic characteristics of the hydrostatic worktable are predicted through simulation of the transformation function by Matlab. The results including influence of the Flow rate ratio, initial flow rate, pump pressure and oil film thickness on the dynamic performance of the hydrostatic worktable are presented and compared with several different series of data.

2. Formulation

2.1. Formulation of the state equation of the hydrostatic table

Force analysis of the hydrostatic guide-way of the worktable is demonstrated in Fig.1. Assuming m is the moving mass of the hydrostatic worktable. A_{e1} and A_{e2} are the effective bearing area of the hydrostatic blocks mounted on the top and bottom surface of the guide-way respectively.

In order to study the influence of the throttle parameters on the dynamic performance of the hydrostatic worktable, several ideal assumptions are made in the hydrostatic bearing system.

The flow state of the hydrostatic oil in the chamber is laminar. The impact of the oil inertia on the dynamic performance of the worktable and the viscosity-pressure effects of the hydraulic oil is ignored. Because the moving speed of the hydrostatic worktable is low, the temperature change caused by friction between the worktable and the oil film is small. The temperature-viscosity effect of the hydrostatic oil could be ignored. The surface of the hydrostatic guide-way is rigid body.

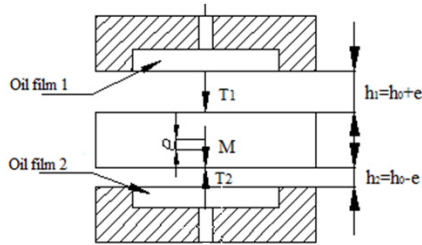


Fig.1 Force Schematic of the closed hydrostatic bearing system

Assume that the initial film thickness of the upper and lower oil chamber is h_0 , as shown in Fig.1. There's no external load acted on the worktable but only its gravity of the moving parts at the beginning. Then the initial liquid resistance of the upper and lower oil chamber can be expressed as

$$R_{10} = R_{20} = \frac{\mu}{Bh_0^3} \quad (2)$$

where μ represents the dynamic viscosity of the hydrostatic oil and B is the anti-flow coefficient of the upper and lower oil chamber, which can be expressed as

$$\bar{B} = \frac{1}{6} \left(\frac{B-b}{l} + \frac{l-l}{b} \right) \quad (3)$$

Through the force schematic of the closed hydrostatic bearing system, one can obtain the force balance equation when there is no load acted on the worktable.

$$mg - p_{10}A_{e1} + p_{20}A_{e2} = 0 \quad (4)$$

where p_{10} and p_{20} represent the initial pressure of the upper and lower oil chamber respectively.

Substituting Eq.(1) into the flow rate equation of the PM controller, the initial flow rate of the upper and lower oil chamber, Q_{10} and Q_{20} can be obtained.

$$\begin{cases} \frac{p_{10}}{R_{10}} = Q_{10} = Q_0 + Q_0(K_r - 1) \frac{p_{10}}{p_s} \\ \frac{p_{20}}{R_{20}} = Q_{20} = Q_0 + Q_0(K_r - 1) \frac{p_{20}}{p_s} \end{cases} \quad (5)$$

Because of the external load acted on the hydrostatic worktable, a small displacement e will be generated. The oil film thickness of the upper and lower oil chamber will be turned into $h_1 = h_0 + e$, $h_2 = h_0 - e$ respectively. Then the liquid resistance of the upper and lower oil chamber can be given by

$$\begin{cases} R_{h1} = \frac{\mu}{B_1(h_0 + e)^3} \\ R_{h2} = \frac{\mu}{B_1(h_0 - e)^3} \end{cases} \quad (6)$$

Taking the small displacement e into account, the new force balance equation can be derived as follow.

$$m\ddot{e} = f + mg - p_1A_{e1} + p_2A_{e2} \quad (7)$$

Combining Eq.4 and Eq.7, one can easily obtain the differential function of the hydrostatic worktable.

$$m\ddot{e} = f - \Delta p_1A_{e1} + \Delta p_2A_{e2} \quad (8)$$

where Δp_1 and Δp_2 represent the pressure difference of the upper and lower oil chamber between initial state and working state of the hydrostatic worktable. $\Delta p_1 = p_1 - p_{10}$, $\Delta p_2 = p_2 - p_{20}$.

Considering the dissolved air mixed in the hydrostatic oil or the air between the restrictor and the oil chamber, the flow into the oil chamber $Q_{chamber}$ is no longer equal to the flow $Q_{controller}$ discharged from the PM controller. The relationship between $Q_{controller}$ and $Q_{chamber}$ can be given by

$$Q_{chamber} = Q_{controller} - Q_{volume} \quad (9)$$

where $Q_{volume} = \frac{V_{oa}}{E} \dot{p}$ represents the volume effect flow and V_{oa} is the volume of the sensitive oil path, E is the elasticity modulus of the hydrostatic liquid.

When external load is exerted on the hydrostatic worktable, the flow discharged from the PM controller can be obtained.

$$\begin{cases} Q_{controller1} = Q_0 + Q_0(K_r - 1) \frac{p_1}{p_s} \\ Q_{controller2} = Q_0 + Q_0(K_r - 1) \frac{p_2}{p_s} \end{cases} \quad (10)$$

As a result, the nonlinear function of the hydrostatic worktable is obtained.

$$\begin{cases} \frac{\mu}{B_1(h_0-e)^3} = Q_{controller1} - A_{b1}\dot{h}_1 - \frac{V_{oa1}}{E}\dot{p}_1 \\ \frac{\mu}{B_1(h_0+e)^3} = Q_{controller2} - A_{b1}\dot{h}_2 - \frac{V_{oa2}}{E}\dot{p}_2 \end{cases} \quad (11)$$

As mentioned above, the nonlinear differential equations represent the relationship among all variables of hydrostatic table guide-way system comprehensively. Expressing in the form of state equation results in

$$\begin{cases} m\ddot{e} = f - \Delta p_1 A_{e1} + \Delta p_2 A_{e2} \\ \frac{\mu}{B_1(h_0-e)^3} = Q_0 + Q_0(K_r-1)\frac{p_1}{p_s} + A_{b1}\dot{e} - \frac{V_{oa1}}{E}\dot{p}_1 \\ \frac{\mu}{B_1(h_0+e)^3} = Q_0 + Q_0(K_r-1)\frac{p_2}{p_s} - A_{b1}\dot{e} - \frac{V_{oa2}}{E}\dot{p}_2 \end{cases} \quad (12)$$

The nonlinear differential equations of the hydrostatic guide-way system are difficult to solve. In order to solve the equation, linearization of the differential equations is carried out in this paper.

2.2. Linearization of the state equation

To obtain the transform function of the hydrostatic worktable through Laplace transform, the nonlinear units of the state equations should be expressed in the form of implicit functions.

$$\begin{cases} \frac{\bar{B}_1 p_1}{\mu}(h_0-e)^3 = l(e, p_1) \\ \frac{\bar{B}_2 p_2}{\mu}(h_0+e)^3 = l(e, p_2) \end{cases} \quad (13)$$

Expressing $l(e, p_1)$ and $l(e, p_2)$ in the form of dualistic Taylor series near the initial points (e_0, p_{10}) and (e_0, p_{20}) results in

$$\begin{cases} l(e, p_1) = l(e_0, p_{10}) + \sum_{i=1}^n \frac{1}{i!} (\Delta e \frac{\partial l}{\partial e} + \Delta p_1 \frac{\partial l}{\partial p_1})^i l(e_0, p_{10}) \\ + \frac{1}{(n+1)!} (\Delta e \frac{\partial l}{\partial e} + \Delta p_1 \frac{\partial l}{\partial p_1})^{n+1} l(e_0 + 9\Delta e, p_{10} + 9\Delta p_{10}) \\ l(e, p_2) = l(e_0, p_{20}) + \sum_{i=1}^n \frac{1}{i!} (\Delta e \frac{\partial l}{\partial e} + \Delta p_2 \frac{\partial l}{\partial p_2})^i l(e_0, p_{20}) \\ + \frac{1}{(n+1)!} (\Delta e \frac{\partial l}{\partial e} + \Delta p_2 \frac{\partial l}{\partial p_2})^{n+1} l(e_0 + 9\Delta e, p_{20} + 9\Delta p_{20}) \end{cases} \quad (14)$$

where $0 < 9 < 1$, $\Delta e = e - e_0$ and $\Delta p_{1,2} = p_{1,2} - p_{01,02}$. Ignoring the high degree polynomial of Eq.13 results in

$$\begin{cases} l(e, p_1) = l(e_0, p_{10}) + (\Delta e \frac{\partial l}{\partial e} + \Delta p_1 \frac{\partial l}{\partial p_1}) l(e_0, p_{10}) \\ l(e, p_2) = l(e_0, p_{20}) + (\Delta e \frac{\partial l}{\partial e} + \Delta p_2 \frac{\partial l}{\partial p_2}) l(e_0, p_{20}) \end{cases} \quad (15)$$

Considering $e_0=0$, one can obtain the linear form of the nonlinear units in the differential function.

$$\begin{cases} \frac{\bar{B}_1 p_1}{\mu}(h_0-e)^3 = \frac{\bar{B}_1 p_{10}}{\mu} h_0^3 - \frac{3\bar{B}_1 p_{10}}{\mu} h_0^2 \Delta e + \frac{\bar{B}_1}{\mu} h_0^3 \Delta p_1 \\ \frac{\bar{B}_2 p_2}{\mu}(h_0+e)^3 = \frac{\bar{B}_2 p_{20}}{\mu} h_0^3 - \frac{3\bar{B}_2 p_{20}}{\mu} h_0^2 \Delta e + \frac{\bar{B}_2}{\mu} h_0^3 \Delta p_2 \end{cases} \quad (16)$$

Substituting Eq.12 into Eq.16 and substituting e, p_1, p_2 with $e_0 + \Delta e, p_{10} + \Delta p_1, p_{20} + \Delta p_2$ respectively, one can obtain the linear state equations of the closed hydrostatic bearing system of the worktable.

$$\begin{cases} m\Delta\ddot{e} = f - \Delta p_1 A_{e1} + \Delta p_2 A_{e2} \\ \frac{V_{oa1}}{E} \Delta\dot{p}_1 + (\frac{\bar{B}_1}{\mu} h_0^3 \Delta p_1 - Q_0 \frac{K_r-1}{p_s}) \Delta p_1 = A_{b1} \Delta\dot{e} + \frac{3\bar{B}_1 p_{10}}{\mu} h_0^2 \Delta e \\ \frac{V_{oa2}}{E} \Delta\dot{p}_2 + (\frac{\bar{B}_2}{\mu} h_0^3 \Delta p_2 - Q_0 \frac{K_r-1}{p_s}) \Delta p_2 = -A_{b2} \Delta\dot{e} - \frac{3\bar{B}_2 p_{20}}{\mu} h_0^2 \Delta e \end{cases} \quad (17)$$

Since $\Delta e(0^+), \Delta e'(0^+), \Delta p_1'(0^+), \Delta p_2'(0^+)$ all equal zero, the Laplace transform of Eq.17 results in

$$\begin{cases} m\Delta E(s)s^2 = F(s) - \Delta p_1(s) A_{e1} + \Delta p_2(s) A_{e2} \\ (\frac{V_{oa1}}{E} s + \frac{\bar{B}_1}{\mu} h_0^3 - Q_0 \frac{K_r-1}{p_s}) \Delta p_1(s) = (A_{b1} s + \frac{3\bar{B}_1 p_{10}}{\mu} h_0^2) \Delta E(s) \\ (\frac{V_{oa2}}{E} s + \frac{\bar{B}_2}{\mu} h_0^3 - Q_0 \frac{K_r-1}{p_s}) \Delta p_2(s) = -(A_{b2} s + \frac{3\bar{B}_2 p_{20}}{\mu} h_0^2) \Delta E(s) \end{cases} \quad (18)$$

Assuming that $F(s)$ is the input of the hydrostatic bearing system, the output, $E(s)$, is the absolute displacement of the hydrostatic worktable in the vertical direction. Finally the transformation function of the hydrostatic worktable is derived,

$$G(s) = \frac{E(s)}{F(s)} = \frac{J^{-1}(I_b s^2 + I_a s + 1)}{I_4 s^4 + I_3 s^3 + I_2 s^2 + I_1 s + 1} \quad (19)$$

where

$$J = \frac{3P_0 A_{e1}}{h_0(1-cR_{10})} + \frac{3P_0 A_{e2}}{h_0(1-cR_{20})}$$

$$I_a = \frac{V_{0a1} V_{0a2} R_{10} R_{20}}{E^2 (1-cR_{10})(1-cR_{20})}$$

$$I_b = \frac{V_{0a1}R_{10}}{E(1-cR_{10})} + \frac{V_{0a2}R_{20}}{E(1-cR_{20})}$$

$$I_4 = m \frac{V_{0a1}V_{0a2}R_{10}R_{20}}{E^2(1-cR_{10})(1-cR_{20})} J^{-1}$$

$$T_3 = mJ^{-1} \left[\frac{V_{0a1}R_{10}}{E(1-cR_{10})} + \frac{V_{0a2}R_{20}}{E(1-cR_{20})} \right]$$

$$T_2 = J^{-1} \left[m + \frac{A_{e1}A_{b1}V_{0a1}R_{10}R_{20}}{E(1-cR_{10})(1-cR_{20})} + \frac{A_{e2}A_{b2}V_{0a2}R_{10}R_{20}}{E(1-cR_{10})(1-cR_{20})} \right]$$

$$T_1 = J^{-1} \left(m + \frac{3\bar{B}_1P_{10}A_{e1}V_{0a2}h_0^2}{E\mu} + \frac{3\bar{B}_2P_{20}A_{e2}V_{0a1}h_0^2}{E\mu} \right) \times \frac{R_{10}R_{20}}{(1-cR_{10})(1-cR_{20})} + J^{-1} \left(\frac{A_{e1}A_{b1}R_{10}}{1-cR_{10}} + \frac{A_{e2}A_{b2}R_{20}}{1-cR_{20}} \right)$$

3. Results and discussion

3.1. Influence of the Flow rate ratio on the dynamic performance of the hydrostatic worktable

Under normal circumstances, when the step response adjustment time of the system is shorter, the dynamic performance of the system is the better [14,15].

The hydraulic oil is VG46, and the dynamic viscosity is $\mu=40.342\text{mpas}$ at room temperature. The top and bottom oil film gaps of the closed hydrostatic guide-way are $30\mu\text{m}$. The total mass of the hydrostatic worktable and the turntable working on it is $m=8\text{t}$. The young's modulus of the hydrostatic oil is $E_{oa}=2\times 10^9\text{Pa}$. The volume of the sensitive oil path is $V_{oa}=300\text{cm}^3$.

Change the value of the restrictor's flow ratio and keep Q_0 , P_p constant. The dynamic response curve of the hydrostatic worktable bearing system can be obtained, as shown in Fig.2.

As shown in Fig.2, the response characteristics of the hydrostatic bearing system are the same under the action of the step load and the responses are transient multi-oscillation processes. But different results of the step response are achieved when the flow rate ratio Q_0 changed. The flow rate ratio of the restrictor affects the overshoot, settling time and the final displacement of the response process. When the flow rate ratio K_r is 5, it needs the longest time for the hydrostatic bearing system to adjust and the maximum displacement and the maximum overshoot arose. When the flow rate ratio K_r is 3, all indicators of the system were improved.

3.2. Influence of the initial flow rate on the dynamic performance of the hydrostatic worktable

The initial flow rate is one of the key parameters of PM controller. When other parameters of the PM controller remain constant, different initial flow rate value corresponds to different system step response. In this paper, the initial flow

rate of restrictor is $10\text{cm}^3/\text{s}$, $12\text{cm}^3/\text{s}$, $16\text{cm}^3/\text{s}$, $20\text{cm}^3/\text{s}$, respectively. The simulation results are shown in Fig.3.

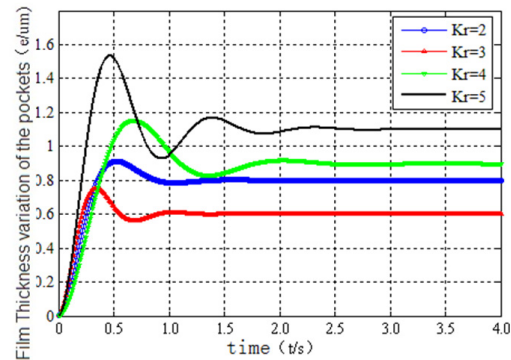


Fig.2. Influence of the Flow rate ratio on the dynamic performance of the hydrostatic worktable

As shown in Fig.3, not the initial flow rate but the overshoot and response time have influence on the final displacement of the bearing system of the hydrostatic guide-way. The overshoot and response time of the hydrostatic guide-way bearing system decrease with increasing initial flow rate from $10\text{cm}^3/\text{s}$ to $16\text{cm}^3/\text{s}$. When the flow rate of the restrictor reaches $20\text{cm}^3/\text{s}$, the overshoot and response time of the hydrostatic guide-way bearing system increase fairly small.

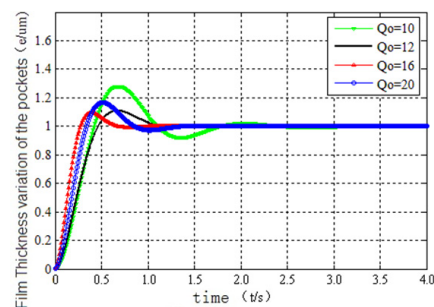


Fig.3. Influence of the initial flow ratio on the dynamic performance of the hydrostatic worktable

3.3. Influence of the pump pressure on the dynamic performance of the hydrostatic worktable

The improved pump pressure can actually increase the pressure inside the oil pocket and further affect the bearing capacity, rigidity and dynamic performance of the system. In this paper, the pump pressure is 0.6MPa , 1.0MPa , 1.4MPa , 1.8MPa and the corresponding step response curve is shown in Fig.4.

As shown in Fig.4, the dynamic performance including the displacement, overshoot and response time, of the system has been improved as the pump pressure increases. The increase of the pump pressure causes that the pressure increases inside the oil pocket and makes the oil flow out quickly. Under the same load condition, the static stiffness of the hydrostatic bearing guide system increases because of the increase of the

pump pressure. So the final displacement of the system decreases when the pump pressure increases.

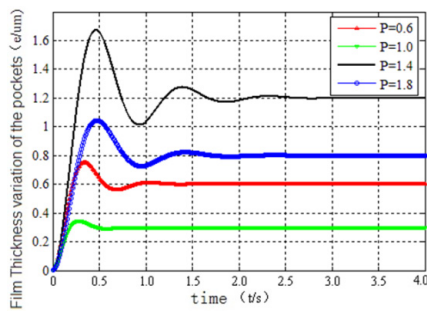


Fig.4. Influence of the pump pressure on the dynamic performance of the hydrostatic worktable

3.4. Influence of the film thickness on the dynamic performance of the hydrostatic worktable

As can be seen from the transfer function of the system, the change of the film thickness affects the dynamic performance of the hydrostatic guide-way bearing system. According to the designed film thickness of the system, the film thickness is selected as $26\text{ }\mu\text{m}$, $28\text{ }\mu\text{m}$, $30\text{ }\mu\text{m}$, $32\text{ }\mu\text{m}$, $34\text{ }\mu\text{m}$. The results are shown in Fig.5.

As shown in Fig.5, the system with the maximum film thickness corresponds to the curve with the maximum displacement. As the film thickness increases, the displacement, adjustment time and maximum overshoot have all increased.

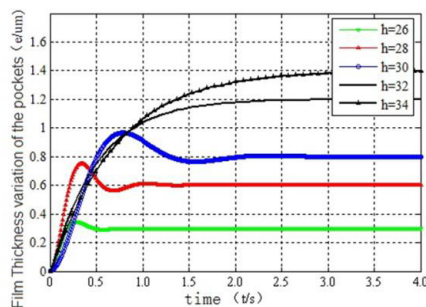


Fig.5. Influence of the film thickness on the dynamic performance of the hydrostatic worktable

4. Conclusion

The transfer function of the hydrostatic bearing system based on the parameters of the PM-controller was derived in this paper. The influences of different parameters of the system were studied and the response curve of step signal was obtained. The simulation results show that the parameters of the hydrostatic bearing system have a big influence on the dynamic performance and a series of optimized parameters is

obtained respectively for the adjustment of the system. When the flow rate ratio K_r is 5, it needs the longest time for the hydrostatic bearing system to adjust and the maximum displacement and the maximum overshoot arose. When the flow rate of the restrictor reaches $20\text{ cm}^3/\text{s}$, the overshoot and response time of the hydrostatic guide-way bearing system hardly increase. The final displacement of the system decreases when the pump pressure increases. The final displacement of the system decreases when the effect of pump pressure increase.

Acknowledgements

This work was financially supported by the Major National Science and Technology Project (2011ZX04004-061).

References

- [1] D.D.Fuller, Theory and practice of lubrication for engineers, John Wiley and Sons, New York, 1956
- [2] M. F. Khalil ,A. S. Ismail. Turbulent lubrication research based on capillary restrictor applied to a ultra-precision machine tool, Tribol. Int.21(1988)249.
- [3] Kazutoshi Katahira, Hitoshi Ohmori, Masahiro Anzai, et al. Development of Large ultra-precision mirror surface grinding machine system with hydrostatic guide-way[J]. Initiatives of Precision Engineering at the Beginning of a Millennium, 2002, (3):794-798.
- [4] OHSUMI T, et al. Characteristic of a hydrostatic bearing with a controlled compensating element[J]. Nippon Kikai Gakkai Ronunshu, 2005,55(512):1084-1089.
- [5] T.D.Pinkus, F.K.Sternlicht. Temperature effect of hydrostatic lead screw with a hydrostatically controlled active restrictor[J]. Bulletin of the Japan Society of Precision Engineering, 2000,24(1):15-20.
- [6] Gao Dianrong, Zhen Dan, Zhang Zuochao. Theoretical analysis and numerical simulation of the static and dynamic characteristics of hydrostatic guides based on Progressive Mengen Flow Controller[J]. Chinese Journal of Mechanical Engineering 2010,23(6):709-716.
- [7] WENFENG LI. Research and design of the hydrostatic guide for DLM series precision lathe machine tool [D].Xi'an Jiaotong University.2011.
- [8] Hu Xinhua, Yang Jilong, Jiang Wei. Dynamic simulation and analysis on oil film of the shipper pair based on hydrostatic support [J]. Machine Tool and Hydrostatics 2003,1:85-88
- [9] Herrbach. U. Dynamic Behavior of hydrostatic slides supplied with pumps for each groove for oil supply. Machine Tool and Hydrostatics 2002,1:185-189
- [10] Xie Peilin, Chen Lie, Duan Xiangyang. Dynamic performance Analysis of a typical hydrostatic journal bearing [J]. China Mechanical Engineering, 2006,16(19):1712-1715.
- [11] Xu Wenqin, Sun Yingda. Probe into the dynamic characteristic of hydrostatic supported column pair [J]. Lubrication Engineering. 2005,4(170):141-146
- [12] Herrbach. U. Dynamic Behavior of Hydrostatic Slides Supplied with Pumps for Each Groove for Oil Supply. Maschinenbautechnik, 1975,24(9):386-392.
- [13] Cheng Hailin, Jiang Wei. The Dynamic Simulation research of Hydrostatic Transformation System Based on Servo-screw Mechanism variable Control[J]. Lubrication Engineering 2004, 2(162):45-48.
- [14] Sinhasan R, Jain S C, Sharma S C. A comparative study of flexible thrust pad hydrostatic bearings with different restrictors[J]. Wear, 1988,121(1):53-70.
- [15] Chen Yansheng. Principle and design of the hydrostatic bearing[M]. Beijing: National Defense Industry Press, 1980.